

Study on the method of mini-jet identification in relativistic heavy ion collisions^{*}

LI De-Sheng(李德胜)¹ TIAN Feng-Ge(田凤革)¹ CHEN Gang(陈刚)^{1,2;1)}

¹ School of Mathematics and Physics, China University of Geosciences, Wuhan 430074, China

² Key Laboratory of Quark & Lepton Physics (Huazhong Normal University),
Ministry of Education, Huazhong 430079, China

Abstract: In this paper a set of methods identifying minijet from final state particles in the relativistic heavy ion collision events is established and the parameter dependence has been investigated in Au+Au collisions at $\sqrt{s}=200$ GeV using a multiphase transport model (AMPT). It is found that the number of minijets reduces with the increasing of collision parameter and raises with the increasing of c.m energy. Furthermore, we analyze the rapidity and momentum distribution inside minijets identified using this method.

Key words: high energy collisions, mini-jet identification, transverse momentum, rapidity

PACS: 13.87.2a, 13.87.Fh **DOI:** 10.1088/1674-1137/35/9/009

1 Introduction

The basic theory of strong interactions—Quantum Chromodynamics (QCD), has two distinct characters: asymptotic free and color confinement. Thus, partons produced in high energy collisions will turn to final flavorless hadrons before being observed. When the virtuality Q of a parton is high enough, the final hadrons will form a taper structure around the direction of the origin parton, which is called a jet. Jets, being experimentally observable, are taken as an efficient way to study the physical properties and interaction dynamics of partons.

In 1975, the two-jets structure was observed in e^+e^- collision experiments at $\sqrt{s} \leq 6$ GeV [1]. This is regarded as an adequate experimental evidence for the existence of partons, which is predicted by the parton models [2]. Theoretically, as the energy increases, the quark-antiquark pairs, moving in the opposite direction may emit a hard gluon with large transverse momentum to form the third jet. In 1979, this astonishing prediction of QCD was confirmed by experiments, when a third jet was observed in e^+e^- collisions at $\sqrt{s} = 17\text{--}30$ GeV, which is considered as the earliest experimental evidence for gluon's exist-

tence [3–6].

In nucleus-nucleus and hadron-hadron collisions, due to the existence of a large background, the situation is more complicated. For the basic theory – QCD remains valid here, jets' production is still anticipated when the collision energy is high enough. In the early 1990s, the production of jets in hadron-hadron collisions was widely studied [7–11] and had been considered as an efficient way to obtain the strong coupling constant α_s [12, 13].

In the last century, nucleus-nucleus collisions were carried out at CERN. However, because the center of mass energy $\sqrt{s_{NN}}$ in those fixed target experiment was less than 20GeV, jets predicted beforehand were not observed. In the beginning of this century, the first relativistic heavy ion collider RHIC at BNL successfully realized Au-Au collision at $\sqrt{s_{NN}}=200$ GeV, jet production became available. In the collisions, the jets were observed to have energy loss when they crossed the central area [14–17], which is called jet quenching. The observation of this phenomenon is regarded as one of the main accomplishments in RHIC experiments; and also it is taken as the implication for the configuration of heat and high density matters produced in relativistic heavy ion collisions [18, 19].

Received 2 December 2010

* Supported by National Natural Science Foundation of China (10775056)

1) E-mail: chengang1@cug.edu.cn

©2011 Chinese Physical Society and the Institute of High Energy Physics of the Chinese Academy of Sciences and the Institute of Modern Physics of the Chinese Academy of Sciences and IOP Publishing Ltd

Thus, the jet is recognized as a powerful tool for studying the properties of the produced new form of matter [20, 21].

Due to the significance of jet physics, in this thesis, we carefully study the methods for selecting minijets and the characters of selected minijets in relativistic heavy ion collisions.

2 The method for selecting minijets

Theoretically [22], the jet is a cone structure formed by a group of hadrons or partons around one certain axis. In high energy hadron-hadron collisions, the jet is generally defined with the cone algorithm [23, 24]. One certain direction is chosen as the jet axis and then the pseudo-rapidity η and azimuthal angle φ plane for a particle are constructed, where η is defined as $\eta = -\frac{1}{2} \ln \tan \theta$ and θ is the angle with jet axis. By defining a radius parameter $R = \sqrt{\eta^2 + \varphi^2}$ for each particle, the particles with $R \leq R_0$ are identified as a jet [25], where

$$\varphi = \arccos \frac{p_x}{p_t}. \quad (1)$$

In e^+e^- collisions, jets are generally identified through some jet-finding processes, e.g the Jade or Durham [26], in which there is a parameter y_{cut} . This relationship between y_{cut} and the cut value of relative transverse momentum $k_{t,\text{cut}}$ [27] is

$$k_{t,\text{cut}} = \sqrt{y_{\text{cut}}} \cdot \sqrt{s}, \quad (2)$$

where \sqrt{s} is the c.m energy. The relative transverse momentum k_t between two particles i and j is defined as [27]

$$k_{t,ij} = 2 \min(E_i, E_j) \sin \frac{\theta_{ij}}{2}. \quad (3)$$

Two particles having a k_t smaller than $k_{t,\text{cut}}$ are grouped into one jet [27].

In relativistic heavy ion collisions, people usually use a high transverse momentum trigger to define a jet and the chosen trigger is called a leading particle. Assume the momentum, transverse momentum, rapidity and azimuth angle of the leading particle are P , p_{t0} , y_0 and φ_0 and take this particle as the jet center; and the momentum, transverse momentum, rapidity and azimuth angle of the around particle i are denoted by p_i , p_{ti} , y_i and φ_i , respectively. The jet is generally considered as a cone structure formed by a group of particles, so the rapidity and azimuth angles, relative to the leading particle, of all particles inside one jet should fall into a certain range. Thus we define the distance between the leading particle

and particle i as follows:

$$R_i = \sqrt{(y_0 - y_i)^2 + (\varphi_0 - \varphi_i)^2}. \quad (4)$$

If we choose a radius cut parameter R_0 to define a cone space, when the distance of i th particle with the leading particle $R_i < R_0$, this particle will fall into this cone space.

In summary, in relativistic heavy ion collisions, the minijets may be selected as the following steps:

1. First, the parameters for selecting minijets, the maximum radius R_0 and the leading particles' minimum transverse momentum P_{T0} , are fixed on.

2. A particle with the largest transverse momentum is selected from all final particles and is considered as the leading particle. The transverse momentum, rapidity and azimuth angle of the leading particle are labeled as p_{t0} , y_0 , φ_0 , respectively. This leading particle is taken as the center to select the particles forming a minijet.

3. According to Eq. (4), the distance R_i between the leading particle and the other particle i is calculated. If $R_i < R_0$, the particle i belongs to this minijet.

The above steps in the remaining particles are repeated until there is no particle with a transverse momentum large enough to be selected as a leading particle.

As an example, a sample event of relativistic heavy ion Au+Au collision at $\sqrt{s_{\text{NN}}} = 200$ GeV is produced by using a multiphase transition model (AMPT) [28] and the minijets are identified using the process mentioned above.

First of all, to analyze the influence of maximum radius, we select minijets when radius R_0 are 0.5, 0.75, 1.00, 1.25, 1.5, 1.75 and 2.0 and the transverse momentum parameter P_{T0} varies from 0.5 to 2.9 GeV, respectively. The results for the numbers of selected out minijets are shown in Fig. 1.

As shown in Fig. 1, the cut parameters significantly influence the selection of minijets. Obviously, if the transverse momentum parameter P_{T0} selected minijet are fixed, the total number of minijet reduces as the cut parameter R_0 increases. Because the sum of particles is definite, with larger R_0 , one jet contains more particles, as a consequence the number of jets reduces. On the other hand, with larger minimum transverse momentum set for leading particles, the number of particles fitting the criteria reduces and it is the same case with the number of minijets. Obviously, in high energy heavy ion collisions, the minijet selection has the dependence on cut parameters. However, when $R_0 \geq 1.5$, $P_{T0} \geq 2.0$ GeV, this

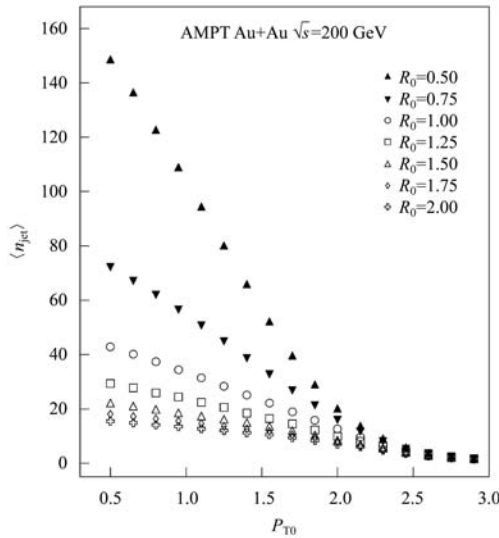


Fig. 1. The variation of the average number of minijets $\langle n_{\text{jet}} \rangle$ with the transverse momentum parameter P_{T0} for AMPT Au-Au collision at $\sqrt{s} = 200$ GeV and the dependence of selected minijets numbers on cut parameters R_0 .

dependence on cut parameters R_0 and P_{T0} will be weakened.

3 The dependence of minijets on energy and collision parameters

Now we apply the above-mentioned minijet-algorithm to analyze the event samples of the relativistic heavy ion Au+Au collision with different values of c.m. energy and collisions parameter b and

study their dependence of the total number of minijets selected from one event on the different value of c.m. energy and collision parameter b . The event samples of different c.m. energy and collision parameter b are constructed from AMPT, respectively, each consists of 1000 relativistic heavy ion Au+Au collision events.

Under the condition for the selection parameters as $R_0 = 1.5$, $P_{T0} = 2$ GeV and $b = 0$, we calculate the average number of minijet selected when c.m. energy equals 20, 40, \dots , 200 GeV, respectively. The result is shown in Fig. 2(a).

In the same way, under the condition for the selection parameters as $R_0 = 1.5$, $p_{T0} = 2$ GeV and $\sqrt{s} = 200$ GeV, we calculate the average number of minijet selected when collision parameter b equals 1, 2, \dots , 8 fm, respectively. The result is shown in Fig. 2(b).

Figure 2(a) shows that the number of minijets raises with the c.m. energy increasing, which is because the higher the collision energy is, the more fierce the collision is, i.e, the number of total particles and leading particles raises. So the number of minijets raises with the c.m. energy increasing.

It can be seen from Fig. 2(b) that the number of minijets reduces with the increasing of collision parameter. This is because that the collision becomes weak when the collision parameter b increases, so the number of total particles and leading particles reduces. Thus the number of minijets reduces as the collision parameter increases.

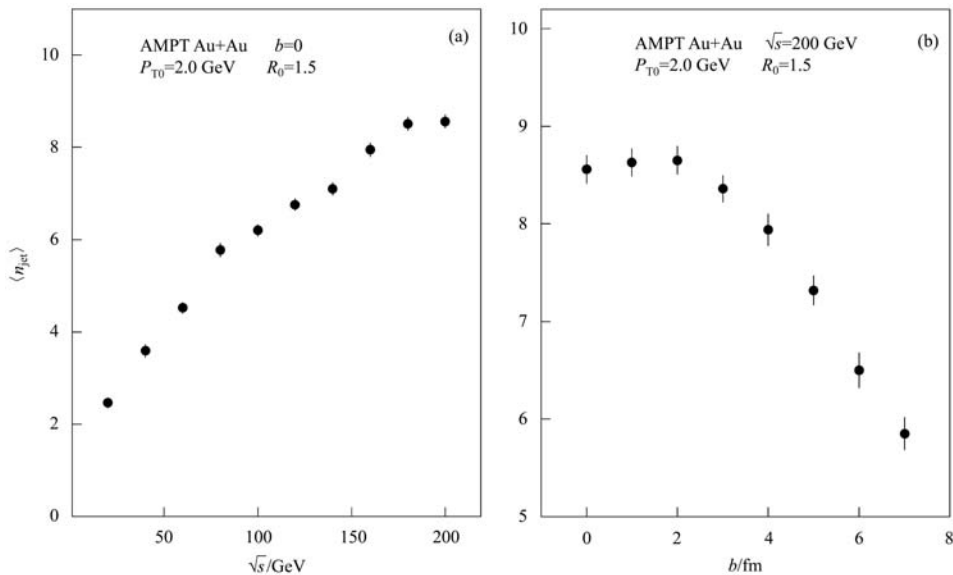


Fig. 2. The distribution of average number of minijets (a) as a function of the collision energy \sqrt{s} at the collision parameter $b = 0$, (b) as a function of the collision parameter b at $\sqrt{s} = 200$ GeV, the data of Au-Au collisions produced by AMPT model.

4 The longitudinal and transverse distributions of particles inside minijets

In order to study the particle distributions inside the minijets, a full event sample of final state particles with 1000 relativistic heavy ion Au+Au collision events at c.m. energy $\sqrt{s_{NN}} = 200$ GeV is generated using AMPT [28]. Then the events subsamples of minijets are determined, using minijet-algorithm given previously selected from the full event sample, with the cut parameters selecting minijets being chosen as $R_0 = 1.5$, $b = 0$, respectively. Then we analyze the variance of rapidity and transverse momentum inside minijets.

First, the momentums of all the particles in the minijet are summed up to p_{jet} , which is defined as the jet momentum. The direction of p_{jet} is defined as the longitudinal direction and the directions perpendicular to it are the transverse directions. The rapidity y and transverse momentum p_t inside the minijet are defined according to these directions as usual.

The rapidity distributions for all particles, charged particles, Kaons and Pions inside a single minijets are shown in Fig. 3, respectively. It can be seen from Fig. 3(a) that the rapidity distributions are distributed over the -4.2 to 4.2 district and most of the particles inside minijets are distributed in the center rapidity range. The number of particles increases sharply from $y = -4$ to -1 , then turns to be an invariant flat until $y = 1$ and quickly decreases as the

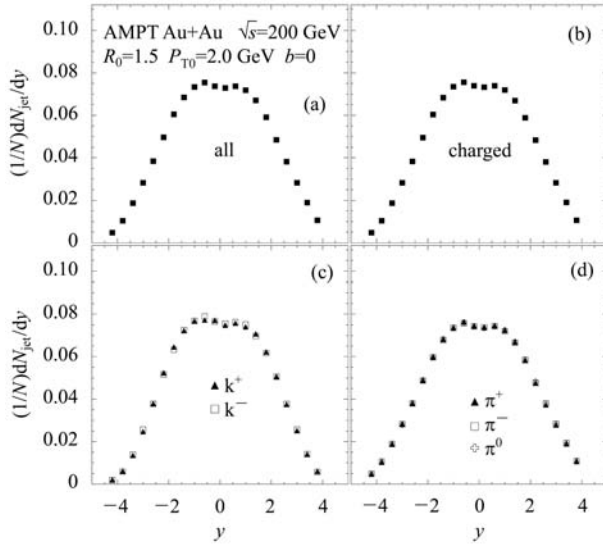


Fig. 3. Rapidity distributions of minijets from Au+Au collision at $\sqrt{s} = 200$ GeV, with cut parameter $R_0 = 1.5$, and collision parameter $b = 0$, (a) all particles, (b) charged particles, (c) K^+ , K^- , (d) π^+ , π^- , π^0 .

rapidity is more than 1. The rapidity distributions inside a single minijet for charged particles, Kaons (K^+ , K^-) and Pions (π^+ , π^- , π^0) shown in Figs. 3(b)–(c), have the similar behavior.

Figure 4 shows the transverse momentum distributions of particles inside a single minijet corresponding to all particles, charged particles, Kaons and Pions, respectively. The transverse momentum distributions increase sharply from $p_t = 0$ until a maximum peak around $p_t = 0.2$ – 0.26 is reached. The transverse momentum distributions of different particle inside a single minijet, shown in Figs. 4(b)–(d), have a similar behavior, which the peak moves rightward with the increasing of mass of particle comparison Fig. 4(c). Contrary to the dependence of transverse momentum distributions on the mass of the particle inside a single minijet, it turns out to be independent on their charge (in Fig. 4(c) or (d)).

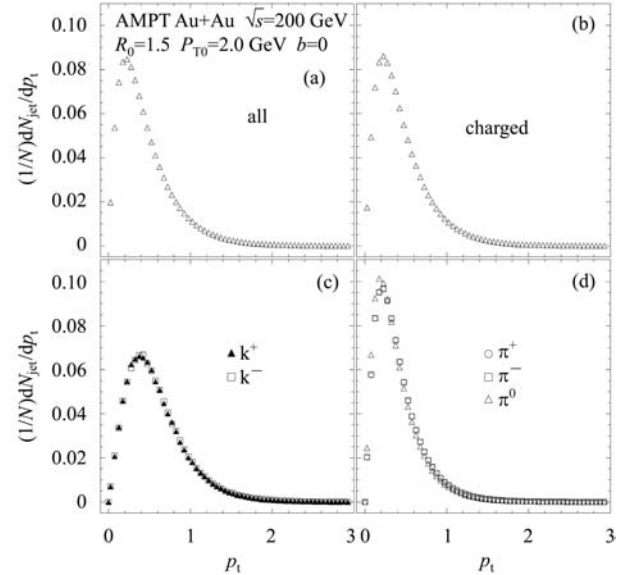


Fig. 4. Transverse momentum distributions of minijets from Au+Au collision at $\sqrt{s} = 200$ GeV, with cut parameter $R_0 = 1.5$ and collision parameter $b = 0$, (a) all particles, (b) charged particles, (c) K^+ , K^- , (d) π^+ , π^- , π^0 .

5 Conclusion and discussion

In this paper we have defined parameters – the relative distance cut parameter R_0 and a set of methods identifying minijets from final state particles in the relativistic heavy ion collision events is carried out. The dependence of this method identifying minijets on cut parameters is studied in relativistic heavy ion Au+Au collision events at $\sqrt{s} = 200$ GeV using AMPT. Obviously, in high energy heavy ion collision

ons, the jet selection has the dependence on cut parameters. As $R_0 \geq 1.5$ and $P_{T0} \geq 2.0$ GeV, this dependence on cut parameters will be weakened. On the other hand, it is found that the number of minijets selected using this method reduces with the increasing of collision parameter and raises when the c.m. energy increases. Furthermore, we have analyzed the distribution properties of rapidity and momentum inside minijets in high energy heavy ion collisions.

It is worth noting that an event consists of large hard scattering and also many soft collisions in the relativistic heavy ion collision. The minijet should originate in the hard scattering. However, we have

selected the minijet which consists of large transverse momentum outgoing hadrons that originate from the large transverse momentum partons and also hadrons that originate from the “soft” or “semi-hard” multiple parton interactions. The existence of such soft interactions causes the number of selected minijets to have errors and the particles inside the minijet not to be pure. The distribution characteristics of particles inside the minijet have a certain uncertainty.

The authors are grateful to Professor Liu Feng from the Institute of Particle Physics in Huazhong Normal University for his beneficial discussion.

References

- 1 Hanson G, Abrams G S, Boyarski A M et al. Phys. Rev. Lett., 1975, **35**: 1609
- 2 Ellis J, Gaillard M K, Ross G G et al. Nucl Phys. B, 1976, **111**: 253
- 3 Brandelik R et al. (TASSO collaboration). Phys Lett. B, 1979, **86**: 243
- 4 Barber D P et al. (Mark J collaboration). Phys. Rev. Lett., 1979, **43**: 830
- 5 Berger CH, et al. (PLUTO collaboration). Phys. Lett. B, 1979, **86**: 413
- 6 Bartela W et al. (JADE collaboration). Phys. Lett. B, 1980, **91**: 142
- 7 LIU M, LIU F, LIU F, LIU L S. HEP & NP, 1997, **21**: 138 (in Chinese)
- 8 Arnisonj G et al. (UA1 collaboration). Phys. Lett. B, 1983, **123**: 115
- 9 Albajar C et al. (UA1 collaboration). Phys. Lett. B, 1988, **309**: 405
- 10 Banner M et al. (UA2 collaboration). Phys. Lett. B, 1982, **118**: 203
- 11 Banner M et al. (UA2 collaboration). Z. Phys. C, 1985, **27**: 329
- 12 Antoniou N G, Argyres E N, Dimitriadis P S et al. Z. Phys. C, 1987, **36**: 461
- 13 Ceradini F. In: Proceedings of 23rd International Conference. Berkeley: High-energy Physics. 1986. CERN-EP-86-142
- 14 Back B B et al. (PHOBOS collaboration). Phys. Rev. Lett., 2003, **91**: 072302
- 15 Adler S S et al. (PHENIX collaboration). Phys. Rev. Lett., 2003, **91**: 072303
- 16 Adams J et al. (STAR collaboration). Phys. Rev. Lett., 2003, **91**: 072304
- 17 Arsene I et al. (BRAHMS collaboration). Phys. Rev. Lett., 2003, **91**: 072305
- 18 Gyulassy M, Plumer M. Phys. Lett. B, 1990, **243**: 432
- 19 Baier R, Dokshitzer YU L, Mueller A H, Schiff D. Phys. Rev. C, 1999, **60**: 064902
- 20 WANG E K, WANG X N. Phys. Rev. Lett., 2002, **89**: 162301
- 21 Vitev I, Gyulassy M. Phys. Rev. Lett., 2002, **89**: 252301
- 22 Sterman G, Weinberg S. Phys. Rev. Lett., 1977, **39**: 1436
- 23 Arnisonj G et al. (UA1 collaboration). Phys. Lett. B, 1983, **123**: 115
- 24 Ellis S D, Kunszt Z, Soper D E. Phys. Rev. D, 1989, **40**: 2188
- 25 Liu(Y) F, LIU F, Mod. Int. J. Phys. A, 1998, **13**: 1969
- 26 Dokshitzer YU L. Phys. G, 1991, **17**: 1481
- 27 Dokshitzer YU L, Leder G D, Moretti S, Webber B R. High Energy Phys., 1997, **8**: 1
- 28 LIN Z W, KO C M, LI B A et al. Phys. Rev. C, 2005, **72**: 064901
- 29 Affolder T, Akimoto H, Akopian A et al. Phys. Rev. D, 2002, **65**: 092002